Chapter Two

Charles J. Neumann
USNR (Retired)
U, S. National Hurricane Center
Science Applications International Corporation

2. A Global Tropical Cyclone Climatology

2.1 Introduction and purpose

Globally, seven tropical cyclone (TC) basins, four in the Northern Hemisphere (NH) and three in the Southern Hemisphere (SH) can be identified (see Table 1.1). Collectively, these basins annually observe approximately eighty to ninety TCs with maximum winds 63 km h^{-1} (34 kts). On the average, over half of these TCs (56%) reach or surpass the hurricane/ typhoon/ cyclone surface wind threshold of 118 km h^{-1} (64 kts). Basin TC activity shows wide variation, the most active being the western North Pacific, with about 30% of the global total, while the North Indian is the least active with about 6%. (These data are based on 1-minute wind averaging. For comparable figures based on 10-minute averaging, see Table 2.6.)

Table 2.1. Recommended intensity terminology for WMO groups. Some Panel Countries use somewhat different terminology (WMO 2008b). Western N. Pacific terminology used by the Joint Typhoon Warning Center (JTWC) is also shown.

<<Previous

Next>>

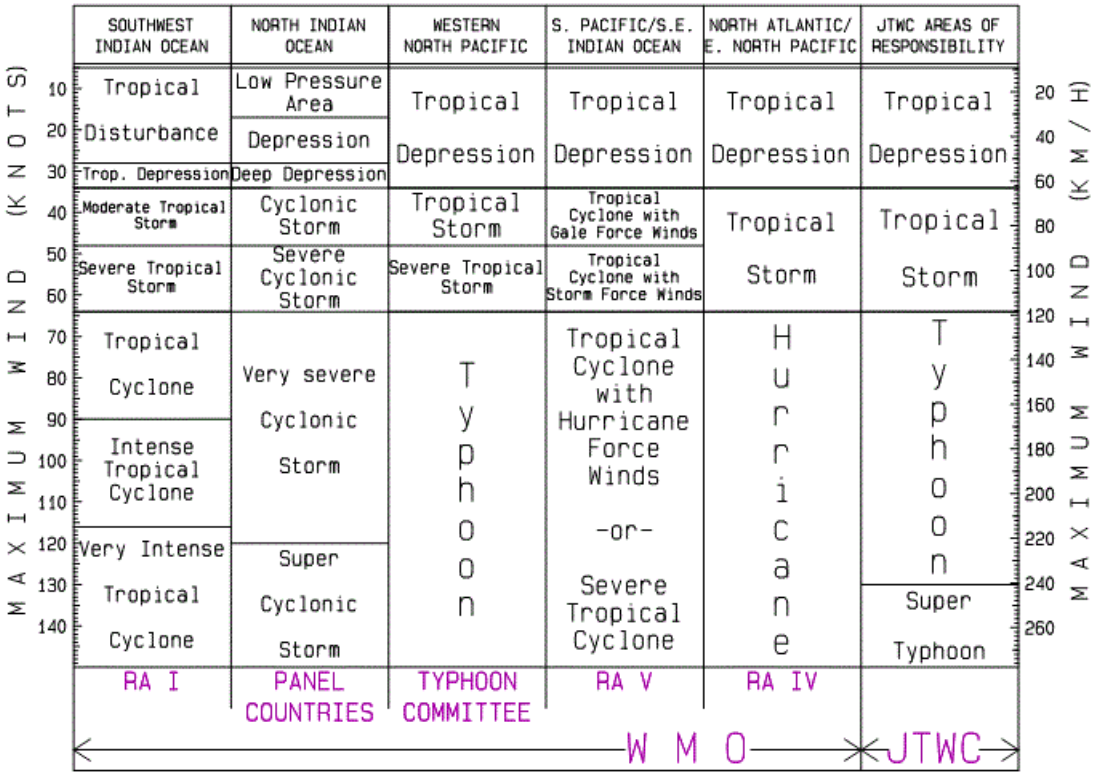

Over the years, many countries subject to these TC events have nurtured the development of government, military, religious and other private groups to study TC structure, to predict future motion/intensity and to mitigate TC effects. As would be expected, these mostly independent efforts have evolved into many different TC related global practices. These would include different observational and forecast procedures, TC terminology, documentation, wind measurement, formats, units of measurement, dissemination, wind/ pressure relationships, etc. Coupled with data uncertainties, these differences confound the task of preparing a global climatology.

While the World Meteorological Organization (WMO), through its Tropical Cyclone Programme (TCP), has taken the lead in standardizing many of these TC procedures, considerable differences remain. Some of these are relatively easy to address. Others, such as wind measurement, are not.

Throughout this chapter, measurement will be given in both English and metric units. However, differentiating between the numerous regional TC intensity (stage) terminologies in textual material is awkward and detracts from readability. Accordingly, intensity stages will be described using WMO Region IV terminology; that is, tropical depressions, tropical storms or hurricanes. Table 2.1, derived from recent WMO publications such as WMO (2008a), provides equivalent terminology for other regions. Tropical cyclones that fail to reach the tropical storm stage will not be included in any of the tables or charts that follow. The main reason for this omission is that documentation of these weaker TCs is inconsistent and highly objective among basins.

<<Previous

Next>>

Each of the seven basins, as defined in Table 2.2 in Chapter 2.1.3, has both unique and common features that relate to TC internal structure, motion, forecast difficulty, frequency, intensity, energy, intensity, etc. The primary purpose of this Chapter is to display all but the first of the above listed features (internal structure) in such a manner that inter- and intra-basin and hemispheric differences and similarities can readily be identified. In keeping with this goal, tabular listings are avoided as much as possible. Due to measurement or estimation uncertainties as well as to different basin definitions of sustained wind, TC intensity will be discussed in other than explicit terms.

A secondary but still important purpose of this chapter is to assess the quality and quantity of the TC data utilized in the construction of the various tables and charts contained herein. It will be shown that the quality of the data is highly variable, being dependent on location and era. Other data-related issues that will be addressed are some of the afore-mentioned dissimilar operational practices at various Centers.

To fill in data voids and to make inferences about extreme values, TC climatological data are often manipulated statistically using parametric and non-parametric methods. Accordingly, with emphasis on shortcomings of the data, some statistical procedures and associated statistical pitfalls will also be discussed.

2.1.1 About historical TC data

Presentation of a global tropical cyclone (TC) climatology is necessarily based on best-track documentation. Therefore, the quality of this climatology will be commensurate with the quality of the best-track data. The amount of information contained in most current best-track formats is limited to storm location and intensity (winds and/or pressures) at 6-hourly intervals (0000, 0600, 1200, 1800 UTC). Such data make it possible to compare basin attributes insofar as they relate to those parameters.

Unfortunately, most best-tracks do not currently address other important surface features of TCs such as size, radius of maximum wind (RMW), radius of various intensity winds, landfall location and time of landfall, etc. This makes it difficult to compare basin-to- basin characteristics of those parameters. Ready availability of such parameters would also enhance TC research efforts such as lowering unexplained variance in wind/pressure relationships (Knaff and Zehr, 2007; Guard and Lander, 1996). Various research and operational interests have noted this best-track deficiency. The World Meteorological Organization (WMO) has prepared and disseminated a comprehensive best-track format, a template of which appears in the various Regional Manuals available at http://www.wmo.int/pages/prog/www/tcp/operational-plans.html.

In regard to data quantity, at least 25 years of best-track data are desirable. In the early 1990's, at which time the first edition of this WMO Guide was in preparation, no long-term global collection of creditable best-tracks, in a common format, was known to exist. Accordingly, the author of Chapter 1 (Neumann, 1993), using the United States National Hurricane Center (NHC)

best-track format, assembled such a data set based on the many existing and often conflicting local data sets available at that time. Although Northern Hemisphere (NH) data were reasonably easy to assemble, the Southern Hemisphere (SH) presented problems and these are described and addressed by Neumann (1999, 2000). Particularly troublesome were the numerous heterogeneities and track discontinuities in SH data.

The structure of the Neumann global data set is different for each hemisphere. For the NH, TC tracks are separately documented for each of the four basins. Thus, a multi-basin TC will appear in more than one set and could, inadvertently, be counted more than once in hemispheric totals. For the Southern Hemisphere portion of the data set, each TC is a single entity and, the basin it occupies is determined by the TC longitude. The U.S. Joint Typhoon Warning Center (JTWC) also treats SH best-tracks in this manner. This avoids the possibility of counting the same TC more than once in hemispheric totals. A disadvantage is that the available periods of record for the various hemispheric basins may be dissimilar.

The Neumann global data set, updated through the 2007 TC seasons, mostly with data from the U.S. Joint Typhoon Warning Center (JTWC) and NHC, is used as the basis for all charts in this study. Tabular data (tables 2.5 and 2.6) include the 2008 seasons. Also, many needed changes, particularly to the early SH data, have come to the attention of the author and these have been incorporated into the files. In the interest of eliminating at least some of the pre-satellite data, the early years (1960-1961 through 1965-1966) for the SH and 1891-1970 for the North Indian basin have not been used for any of the graphical or tabular presentations.

2.1.2 On the quality of TC data

The global warming issue has focused attention on the adequacy of archived TC data for detecting secular trends in TC frequency, intensity, landfall, length of season, etc. Data quality is a diverse issue and difficult to assess on a global scale. In general, the quality improves with time and early data is more reliable in the Northern Hemisphere. Polar orbiting weather satellites, in a research mode, were first launched by NASA in 1960 but were not declared operational until 1965. Thus, for the period, 1960-1965, satellite documentation was very fragmented. Even after the 1965 operational era began, it took many years for some Centers to take full advantage of this new TC viewing platform and to develop the expertise to associate satellite signatures with storm position and intensity. Subjectively, problems still exist in this regard.

For the North Atlantic and western North Pacific basins, aircraft TC reconnaissance began in the mid-1940's and became routine in 1946. Such reconnaissance continues and has been expanded in the Atlantic, but was discontinued for the western North Pacific in 1987. Although this platform provided needed ground-truth, early flights were made only once or twice a day, assuming the TC was within the operational range of the aircraft. Intensity changes or peak intensity could easily have been missed. In U.S. Navy Atlantic and western North Pacific aircraft reconnaissance of the 1940's and early 1950's, surface wind speed and direction were subjectively based on visual sea-state conditions, made from altitudes of 400 to 600 feet

(Neumann, 1952). In this connection, Neumann (1996) describes a 1940's era Navy reconnaissance policy of limiting maximum typhoon surface winds to 120 knots. Navigational aids of that era, particularly in the Pacific, were poor and the position of an aircraft in the eye of a TC as well as communication with ground personnel was often very uncertain. This early aircraft reconnaissance is incomplete in contrast to current capabilities.

In addition to TC observational deficiencies, there was little official interest or coordination in the TC documentation issue for the years following WW II. Even after the introduction of computers, transferring TC data to punch cards was laborious, of a low priority and lacking standardization. In the United States, the TC needs of the United States Space Program focused attention on this TC documentation deficiency and prompted Hope and Neumann (1968) to structure a best track file for the Atlantic basin, known as HURDAT. The introduction of computer graphics in the early 1970's and personal computers in the mid-1980's and the World Wide Web greatly simplified compilation and error checking of best-track files.

Before the satellite and aircraft reconnaissance eras, the location and intensity of a tropical cyclone were based largely on chance encounters with ships or populated landmasses. These observations were quite fragmented and meteorological expertise, if available, was required to "connect the dots." Some storms were not detected until several days after their formation or not at all. Thus, the data on individual storms leaves much to be desired. However, in the collective sense, there is valuable information in historical tracks.

In general, the location of a TC is more reliable than is the intensity. Indeed, early TC documentation either lacked intensity or used an *intensity code* (i.e., depression, tropical storm or hurricane). Maximum intensity is particularly uncertain and, even if accurate, may not be documented if a maximum occurred between 6-hourly synoptic times used in best-track files. Also, there is a greater chance of biases in the estimation of intensity. For this reason, other than for the distinction between storm stages (hurricanes, tropical storms, etc.), the charts contained in this chapter (Figs. 2.7 through 2.10) do not explicitly address maximum intensity.

Because of the aforementioned recent widespread intrest in global TC frequency and intensity trends, considerable effort is being focused on the improvement of historical TC best-track data. Harper, et al. (2008) conclude that maximum winds for the early years of the Neumann (1999) global data set, being based largely on early Bureau of Meteorology (BoM) and JTWC data, are too low in the Australian area. Also, a welcome new global data set, International Best Track Archive for Climate Stewardship (IBTrACS)(Kruk et al., 2008) has been assembled, see http://www.ncdc.noaa.gov/oa/ibtracs/. Additionally, Landsea, et al., (2003) describe an extensive ongoing project to revise Atlantic best-tracks back to the year 1851 (HURDAT). Efforts are also underway to re-evaluate historical satellite photos. As pointed out earlier, augmented best-tracks or best-track supplements are needed to document additional TC parameters.

2.1.3 Basin boundaries

Basin bounds used in this study are given in Table 2.2. For the NH, four clusters (see Fig 2.1) of tropical cyclone activity are clearly identifiable: the N. Atlantic, eastern N. Pacific, western N. Pacific and the North Indian (Bay of Bengal and Arabian Sea) basins. For the SH, such clustering is not obvious and the determination of a basin bound is based on other considerations.

The Cape York Peninsula at longitude 142°C is often taken as the bounds between the Australia/southeast Indian and the Australia/southwest Pacific basins. From Fig. 2.4, it can be noted that the average motion of TC's east of this longitude exhibit more of an easterly component while those to the west exhibit a westerly component. Also, from Fig. 2.2, there is somewhat of a minimum of activity at this longitude.

In regard to the bound between the southwest and the southeast Indian Ocean, given as 100°E in Table 2.2, the WMO official high seas warning area between Perth/Jakarta and RSMC La Rèunion is at 90°E. However, from Fig. 2.2, a minimum of TC activity is seen to occur 100°E to 105°E and such minima are typically used to define basin bounds. As a compromise, 100°E will be used here as the basin bound even though it differs somewhat from the WMO forecast responsibility bound of 90°E. Also, the central North Pacific (140°W, westward to 180°) is referred to as the central North Pacific basin with an RSMC in Honolulu. Although TC's, such as INIKI in 1992, do develop in this basin, it will be considered here as part of the eastern North Pacific basin.

Table 2.2. Geographical bounds of the TC basins used in this study. The Eastern and Central N.Pacific are combined into a single basin.

Northen Hemisphere

North Atlantic	Eastern N. Pacific / Central N. Pacific	Western N. Pacific	North Indian
N. Atlantic, Caribbean Sea & Gulf of Mexico	West coast of North America to 140°W 140° to dateline	Dateline to Asia	Bay of Bengal & Arabian Sea

Southern Hemisphere

SW Indian	Australian / SE Indian	Australian / SW Indian
<100°E to Africa	100°E to 142°E	142°E to 120°W

2.1.4 Wind averaging times

A major problem arises when dealing with global tropical cyclone intensity: different sustained wind averaging times are being used by various Centers. U.S. interests use 1-minute averaging while, as sanctioned by the WMO, most other interests use 10-minute averaging. (Two and three minute averaging has been used in portions of some basins.) The average wind is inversely proportional to the averaging time and a near-coastal inland wind averaged over 10 minutes (600 seconds) is about 88% (BoM, 1978, Murnane, 2004) of the wind averaged over 1-

<<Previous Next>>

minute (60 seconds) such that $V_{600}=0.88V_{60}$ or $V_{60}=1.136V_{600}$. Thus, a hurricane having a maximum wind of 120 km h^{-1} (65 knots) in the 1-minute system, would only be a maximum wind of 106 km h^{-1} (57 knots) in the 10-minute system and would be designated as a tropical storm or equivalent rather than a hurricane or equivalent. Additional discussion on this topic can be found in Murnane (2004).

Table 2.3 provides additional insight into the wind-averaging dilemma. To simulate 10-minute averaging, all best-track sustained one-minute winds for the North Atlantic (ATL), eastern North Pacific (EPC) and western North Pacific (WPC) were multiplied by 0.88. Referring to the table, it can be noted that, over the 42-year period for the Atlantic basin, there were 470 TCs designated as tropical storms and 261 as hurricanes. However, after the simulated conversion to the 10-minute system, there were 454 TCs reaching the tropical storm threshold (a 3.4% reduction) and only 191 reaching the hurricane threshold (a 26.8% reduction) for that basin.

Table 2.3. The effect of wind averaging time on defining TC stages. Period of record is 1966-2007.

	Number of TCs			
	ATL	EPC	WPC	ALL
At least 63 km h^{-1} (34kts) in 1-min system	470	666	1120	2256
At least 63 km h^{-1} (34kts) in 10-min system	454	619	1064	2137
% difference ((1-min - 10-min)/1-min)	3.4	7.1	5.0	5.3
At least 118 km h^{-1} (64kts) in 1-min system	261	364	716	1341
At least 118 km h^{-1} (64kts) in 10-min system	191	301	615	1107
% difference ((1-min - 10-min)/1-min)	26.8	17.3	14.1	17.4

The general conclusion from the data given in Table 2.3 is that the different averaging times have a significantly greater effect on reaching the hurricane threshold than reaching the tropical storm threshold. From best-track files in the 10-minute system, it can be noted that many TCs have maximum winds of 110 km h^{-1} (60 kts) and would be designated as tropical storms or the equivalent. As pointed out earlier, these would be designated as hurricanes in the 1-min system. Other factors, such as satellite interpretation, wind-pressure relationships and measurement errors also enter into the picture. In reality, the preciseness of the various wind definitions far exceeds the ability to measure or estimate wind with that precision. Nonetheless, standardization of the timing would further clarify the TC wind issue.

2.2. Chart preparation

Excluding TC's that failed to reach an intensity of 34 kts (63 km h^{-1}), Figs. 2.1, 2.2, and Figs. 2.4 through 2.6, depict tropical cyclone frequency and/or motion on a global scale. With some exceptions, these are typically TC's named by one of the WMO Regional Specialized Meteorological Centers (RSMC's). In some, cases, however, a post-analysis had indicated a TC

did reach the tropical storm threshold and was later included in the season summary, but without a formal name. In summaries, these are often designated as not named or unnamed. For the Atlantic basin, charts also include some unnamed storms designated as sub-tropical (McAdie et al., 2008).

For Figs. 2.4, 2.5 and 2.6, the analyses are based on a 60 nm grid system having 331 points in the zonal direction and 143 meridionally. Each grid point represents a scan-circle centered on the grid-point. Thus, if the scan-circle radius is over 30 nm, the circular areas will overlap in both the zonal and meridional directions, providing some smoothing to the data. As shown by Taylor (1986), the use of circular rather than square or rectangular scan areas such as latitude/longitude "squares" is a non-biased method of areal tabulation.

For Fig. 2.2, a 75 nm (140 km) scan-radius was used. For a typical TC landfall, this distance approximates the extent of at least minimal damage or concern. For the other global charts involving motion, the scan distance was increased to twice this amount so as to provide additional sample sizes and smoothing. As illustrated by Xue and Neumann (1984a and 1984b), TC's from each basin were passed through the global grid system and counts or sums of various TC parameters were made. For this purpose, the 6-hourly best-track anchor points were interpolated to 1-hourly points using the method of Akima (1970). If more than one hourly point was contained within a grid-zone, only a single average value was retained. This prevents a bias toward slower moving TC's.

2.2.1 Tropical cyclone tracks

Figure 2.1 presents a 10-year display of global TC tracks and considerable variation in track characteristics is evident. Some of these differences are due to different documentation procedures at the various Centers. For example, NHC best-tracks include early portions of the TC extratropical stages (dashed tracks on Fig. 2.1). Other track differences are due to environmental factors such as sea-surface temperature (SST), steering patterns, topography, etc. Additional detail on global tropical cyclone motion is provided by Elsberry (1987).

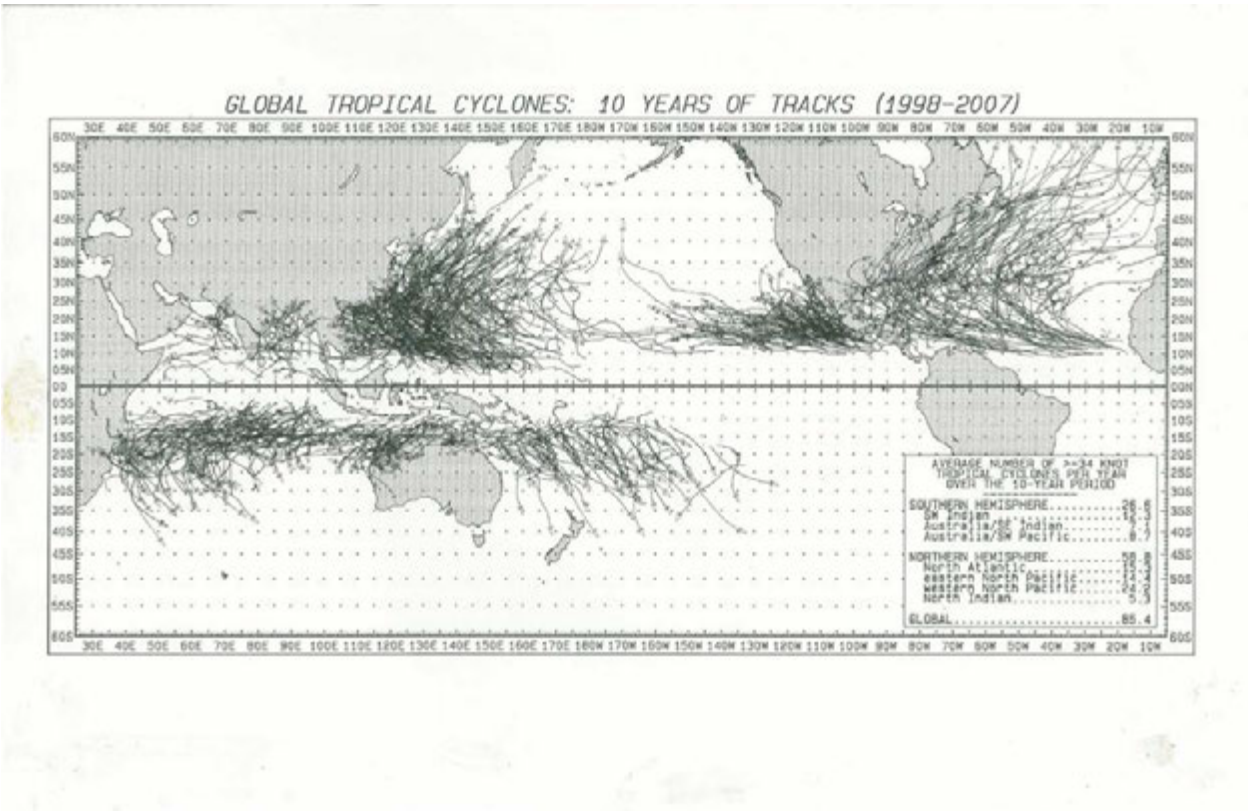

Figure 2.1. Global TC tracks 1998-2007. (click image for full size in new window).

The inset to Fig. 2.1 gives the 10-year totals for each basin and hemisphere. By far the biggest change in these totals from the 10-year 1980-1989 period used in the previous edition of this Guide was for the N. Atlantic where the average annual number of TC's increased from 9.3 to 15.3.

In the eastern North Pacific, TC's typically encounter cold SST's (less 22.5°C) at low latitudes (Frank, 1987) and dissipate before recurvature into the westerlies. By comparison, relatively warm SST's in the western N. Pacific and the N. Atlantic allow many TC's to be sustained well poleward, even after recurvature into the westerlies.

Southern Hemisphere SST's, on the average, are lower than those for given latitudes in the NH. This, together with the more equatorward extent of the SH westerlies, typically result in poleward moving tropical cyclones losing their warm-core characteristics at lower latitudes than for otherwise similar systems in the NH.

All basins observe TC tracks that are anomalous in regard to location, intensity or duration. On rare occasions, for example, eastern North Pacific TC's affect the extreme southwestern portions of the United States (Chenoweth and Landsea, 2004). Other anomalous TC's for other basins include 1989 typhoon GAY that brought extreme damage to both Thailand and India; North Indian 2008 Cyclone NARDIS that devastated southern Myanmar; 1974 Cyclone TRACY that hit Darwin, Australia; and Cyclone LEON-ELINE that brought considerable damage to

<<Previous Next>>

Madagascar, Mozambique and Zimbabwe in 2000. Still other examples would be the 33-day duration of North Atlantic Hurricane GINGER in 1971, the 870 hPa surface pressure of Typhoon TIP in the western North Pacific in 1979 or the development of Hurricane INIKI, 1992 in the central North Pacific. Numerous other examples of anomalous and noted TC's could be cited.

TC's are sometimes evaluated according to their destruction potential and several indices have been introduced. One such index (Bell, 2000) is referred to as Accumulated Cyclone Energy (ACE) and is a function of all of the 6-hourly sustained winds (v) ≥ 34 kts (63 km h^{-1}) over the life of the storm: [$ACE=10^{-4}\Sigma(v^2)$]. Multiplying by 10^{-4} reduces the sum to a more manageable level. Since ACE is dependent on the size of the basin, its use, without size normalization, is mainly for evaluating damage potential in single basins.

Table 2.4 gives average ACE values for the 10-year period used in Fig. 2.1. ACE does not address other destructive factors such as landfall frequency or storm surge. For example, even though the North Indian basin has the lowest ACE average, it has the highest death rate from storm surges. In this connection, Powell and Reinhold (2007), with comments by Hsu and Blanchard (2008), suggest an integrated kinetic energy (IKE) index that addresses this deficiency. *For additional information on ACE, see* http://models.weatherbell.com/tropical.php

Table 2.4. Average ACE values 1988-2007.

North Indian	Aus/SE Indian	Aus/SW Pacific	Eastern N.Pacific	SW Indian	North Altanic	Western N.Pacific
20	40	63	100	104	158	297

2.2.3 Tropical cyclone track density

Visual inspection of the TC tracks displayed in Fig. 2.1 suggest that both the eastern and western N. Pacific have the largest local TC concentration (number per unit area) for a given time interval. Figure 2.2 quantifies this parameter where the unit of measurement is the number of tropical storms or hurricanes per 100 years passing within 75 nmi (140 km) from any point. As previously mentioned, this distance approximates the extent of at least minimal damage from an average TC making landfall. The contours on Fig. 2.2 are based an objective analysis of the 60 nmi (331 x 143) grid, each grid point being an overlapping 75 nmi radius scan circle (Taylor, 1986; Xue and Neumann, 1984a, 1984b).

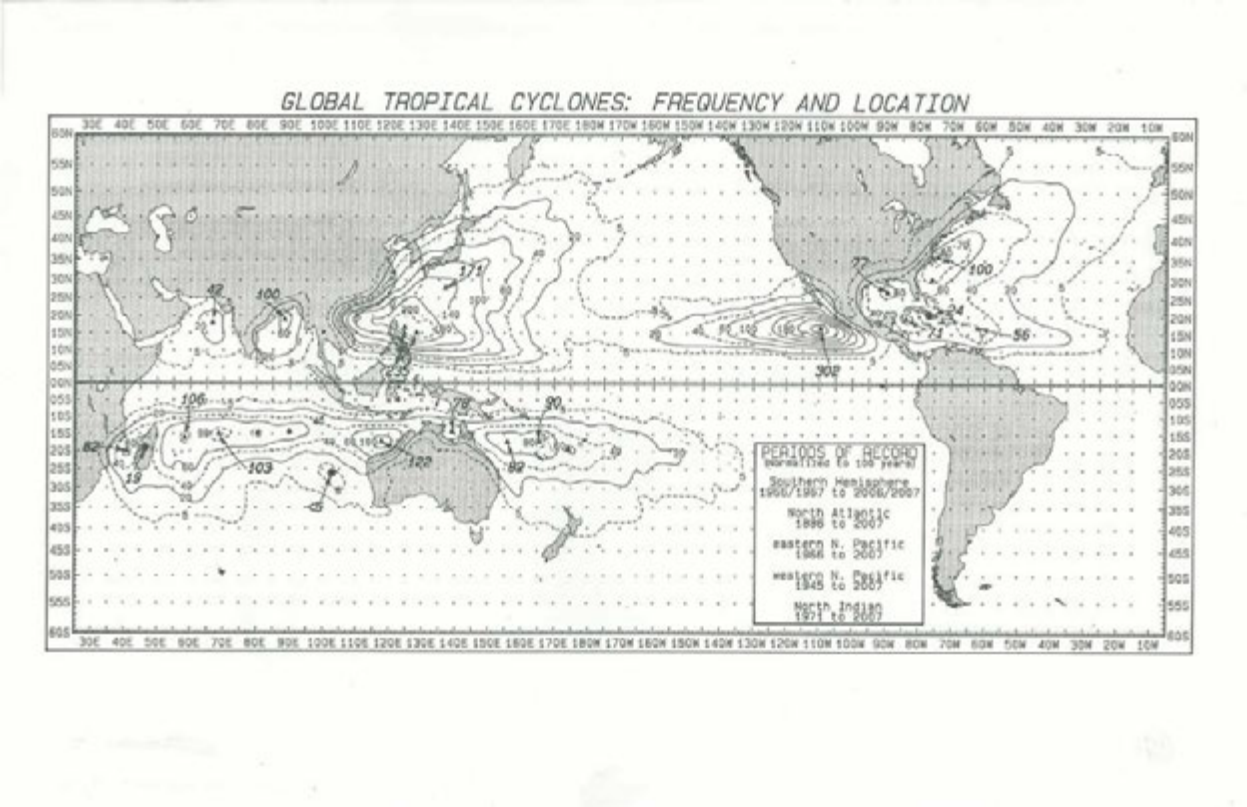

Figure 2.2. Global TC frequency (storms per hundred years). (click image for full size in new window)

The maximum climatological TC density (302 per 100 y or 3.02 per year) occurs in the eastern N. Pacific near 17.2°N, 109.5°W. This is near Isla Socorro (18.8°N, 111.0°W). Another substantial concentration occurs east of Luzon in the Philippine Sea. The highest SH frequency (122 per 100 y) is located off northwestern Australia. Local minima (dark circles on the figure) occur over Madagascar, over eastern Cuba and off the central west coast of Australia. These maximum/ minimum values are somewhat dependent on the grid-point interpolation and smoothing methodology.

The use of a 100-year statistic, as was done in Fig. 2.2, has a number of advantages. It allows combining different periods of record for different basins. Also, it provides convenience in using the Poisson distribution (see Section 2.6.1) to estimate probability of discrete events such as the probability of no TC's passing within 75 nmi of the location of the eastern N. Pacific maximum in any given year. Using the procedure described in Xue and Neumann (1984a), the percent probability of this event is $e^{-3.02}$ x 100 = 4.9% of the 42 years (1966-2007) or 2.05 event occurrences. This is in agreement with observations since the event did not occur for the years 1970 and 1993.

2.2.4 Motion parameters

<<Previous

Next>>

Before introducing global charts of TC motion, a discussion of motion terminology as used on the charts will be presented. TC motion, being a vector quantity, is difficult to describe in the univariate sense. This is illustrated in Fig. 2.3. The figure compares motion characteristics of 22 TC's passing within two of the scan-circles described in section 2.2.1. The upper panel uses data from a region where motion can be described as highly variable while the lower panel does likewise for a region where motion is relatively consistent.

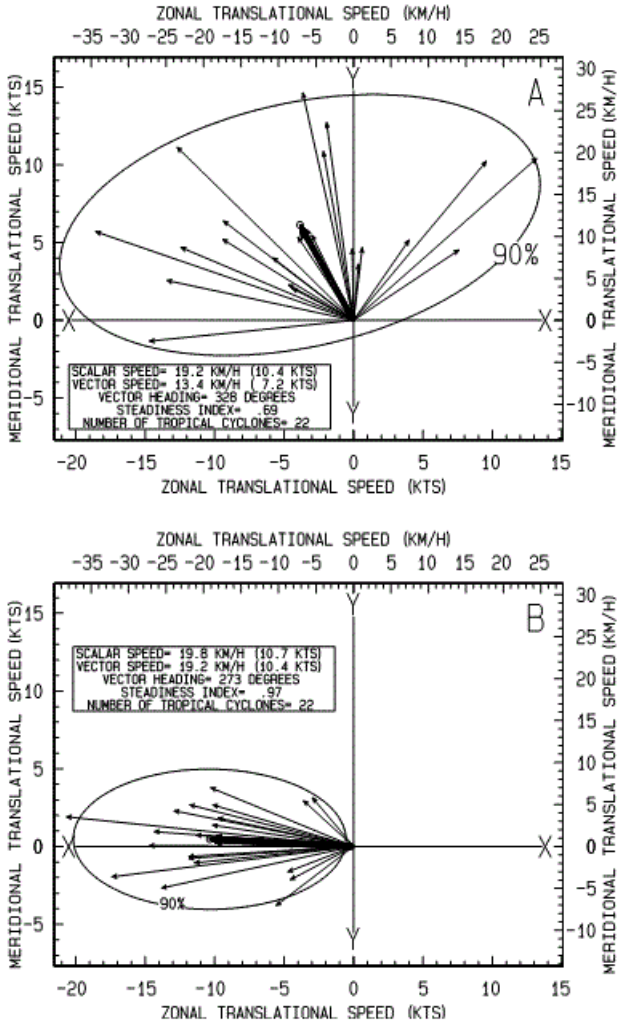

Figure 2.3. Illustration of motion parameters discussed in text. Examples are from two areas with contrasting motion: (a) recurvature zone of western N. Pacific basin and (b) southern portion of eastern N. Pacific basin.

In the X, Y coordinate system, the small arrows depict the end points of each individual motion vector as the TC passes through one of the grid point scan-circles. The average length of these 22 individual vectors, regardless of direction, is defined as the average scalar speed. A *centroid* (small circle on the charts) is obtained by summing and averaging the mathematically signed individual u- and v-components of motion. The length of the bold vector, extending from the X, Y origin to the centroid represents the mean vector speed and the angle (measured

<<Previous Next>>

clockwise from north) is the mean *vector direction* or heading. Collectively, they are referred to as mean *vector motion*.

The bivariate normal distribution (Crutcher et al., 1982) is often used to describe bivariate quantities such as wind, tropical cyclone motion, TC forecast errors, etc. Using this distribution at the two contrasting TC motion sites, Fig. 2.3 displays the theoretical elliptical envelope containing 90% of the vector end-points. The size and shape of the elliptical area reflects the standard deviation of the components of motion as well as the linear correlation between the (X, Y) components. The latter become zero along a new rotated (X', Y') ellipse axes (not shown) through the centroid and random selections from the two marginal distributions can be made along this rotated system.

The ratio of the vector speed divided by the scalar speed provides a measure of motion variability, often referred to as steadiness or a steadiness index (Hope and Neumann, 1971; Crutcher and Quayle, 1974). The higher the ratio, the steadier will be the motion and the highly unlikely value of 1.0 would only be attained if all TC's moved with the same speed and direction. Somewhat arbitrarily, steadiness indices of <0.75, 0.75 to 0.90 and >0.90, are defined here, respectfully, as highly variable, intermediate and relatively steady motion. These values are somewhat different than previously used and were based on the desire to contain about the same number of cases in each of the three motion classification bins used on the global charts. With these criteria, the upper panel in Fig. 2.3, having a steadiness value of 0.69 is described as highly variable and the lower panel, having a steadiness index of 0.97, is described as relatively steady.

2.2.5 TC vector direction

Continuing with a discussion of the global motion charts, the arrows in Fig. 2.4, as illustrated in Fig. 2.3, only represent the average vector direction of TC motion. This is a reflection of the large-scale atmospheric steering patterns. In some areas, these patterns are modified by local influences such as topography (Brand and Blelloch, 1974; Yeh and Elsberry, 1993; Zehnder, 1993). Although the scale of Fig. 2.4 is too crude to show these mesoscale features near Taiwan, they are identifiable around mountainous Madagascar and the extreme southwestern Gulf of Mexico where TC's are deflected to the left by the Sierra Madre mountains of Mexico.

Mean vector motion, by itself, is a rather frail statistic in that it fails to address speed or motion variability. The length of the arrow could be made proportional to speed as is done on Figs. 2.7 through 2.10 but this is difficult to display on such a small-scale map and does not address the motion variability issue.

The colored shading in Fig. 2.4 does provide some insight into motion variability. In the previous section, it was pointed out that steadiness indices of <0.75 are associated with highly variable motion; 0.75 to 0.90 with intermediate motion and >0.90 as relatively steady motion. On Fig. 2.4, it can be noted that the Southern Hemisphere contains little of the "relatively steady" motion. Indeed, much of the motion is designated as "highly variable". In the Northern

Hemisphere, highly variable motion is primarily confined to the recurvature zones. Mostly "relatively steady" motion is noted in the eastern North Pacific basin.

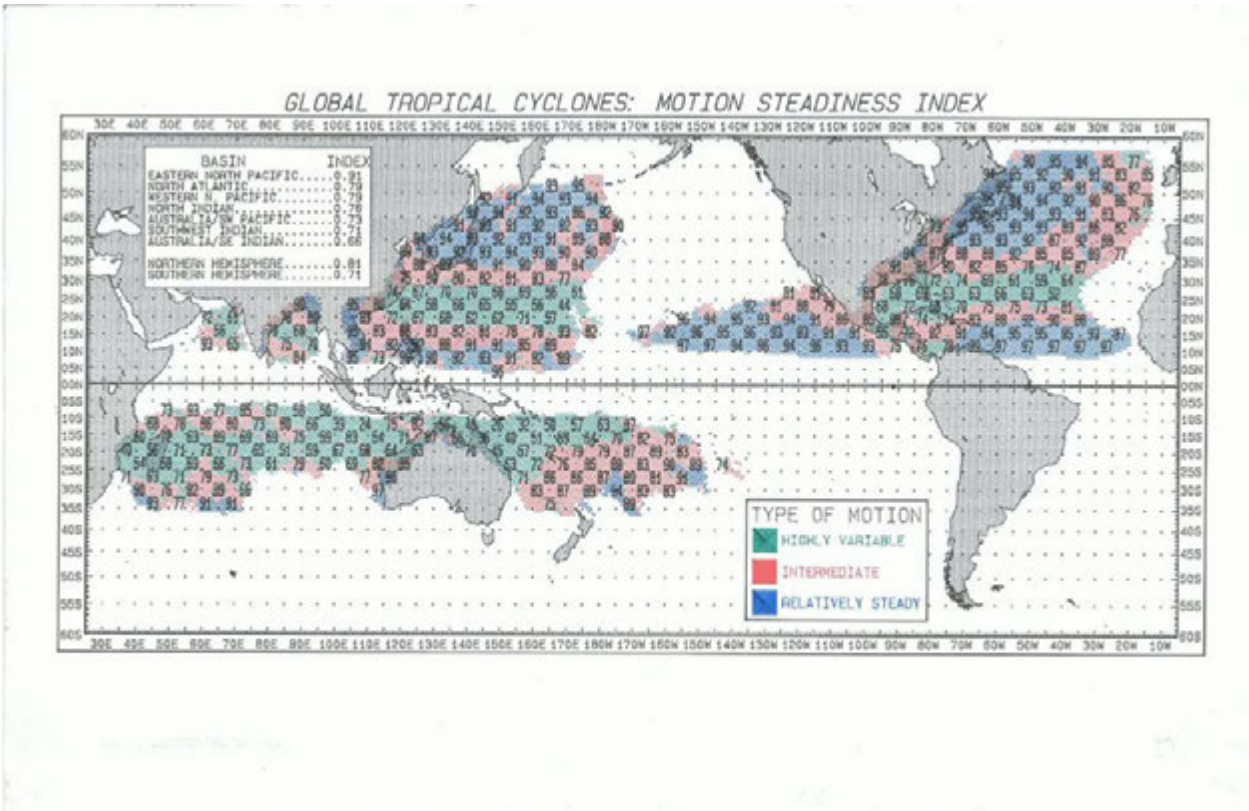

Figure 2.4. Motion steadiness index. (click image for full size in new window)

2.2.6 Vector and scalar speeds

Fig. 2.5 gives global vector and scalar translational TC speeds. These are presented in the "steadiness index" mode (vector speed divided by scalar speed). Three classes of scalar speeds are somewhat arbitrarily defined as slow, medium and fast with specific delimiting values being defined in the figure inset. Slower translational speeds are noted over the SH. As discussed in section 2.2.2, the limited poleward penetrations of Southern Hemisphere TC's contribute to the lack of "fast" motion in that hemisphere. Also noted are the "slow" speeds over the North Indian basin. Both the North Atlantic and the western North Pacific basins exhibit a classical pattern of slower translational speeds during recurvature with much higher speeds poleward and somewhat higher speeds equatorward.

<<Previous

Next>>

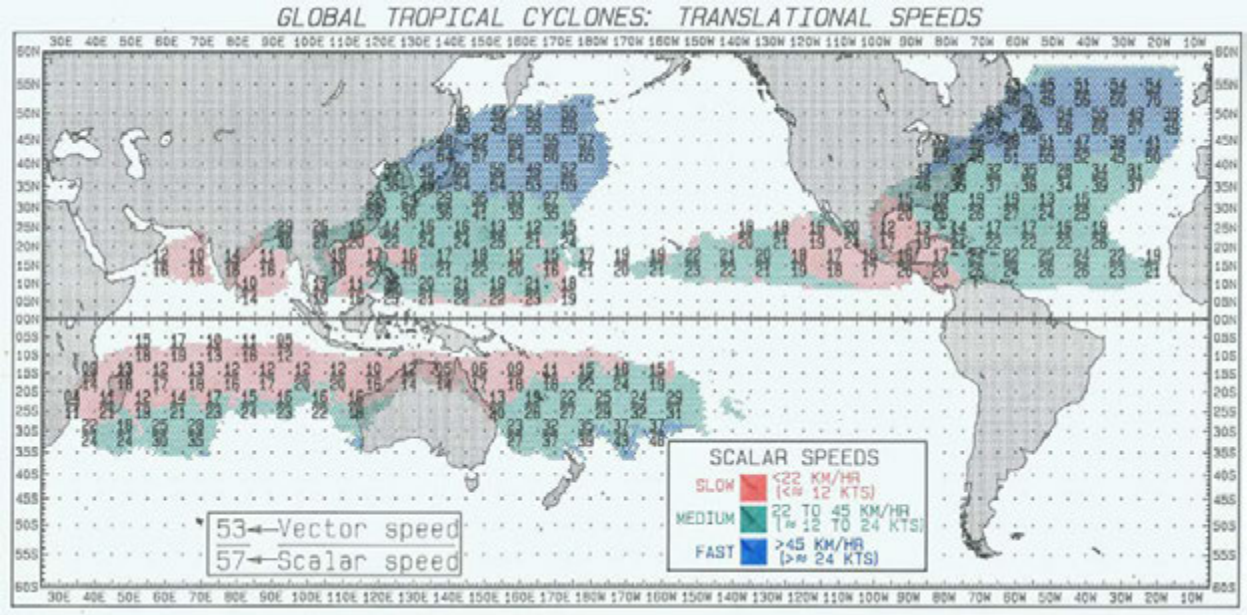

Figure 2.5. Translational TC speeds (vector speed divided by scalar speed).

2.2.7 Global values of the steadiness index

Fig. 2.6 gives global values of the steadiness index (SI) multiplied by 100 and wide variability can be noted. Compared to the NH, many more low values of the SI are noted in the SH, particularly in the Coral Sea area east of Queensland, Australia and off the northwestern coast of Western Australia, where some values are <50. In the NH, highest SI values are found over the eastern N. Pacific basin with some values being as high as 97. The upper left inset gives average steadiness indices for each basin and hemisphere. As would be expected from visual inspection of Fig.2.6, lowest values are found over the SH in the vicinity of Australia and the highest steadiness values are found over the eastern N. Pacific.

<<Previous

Next>>

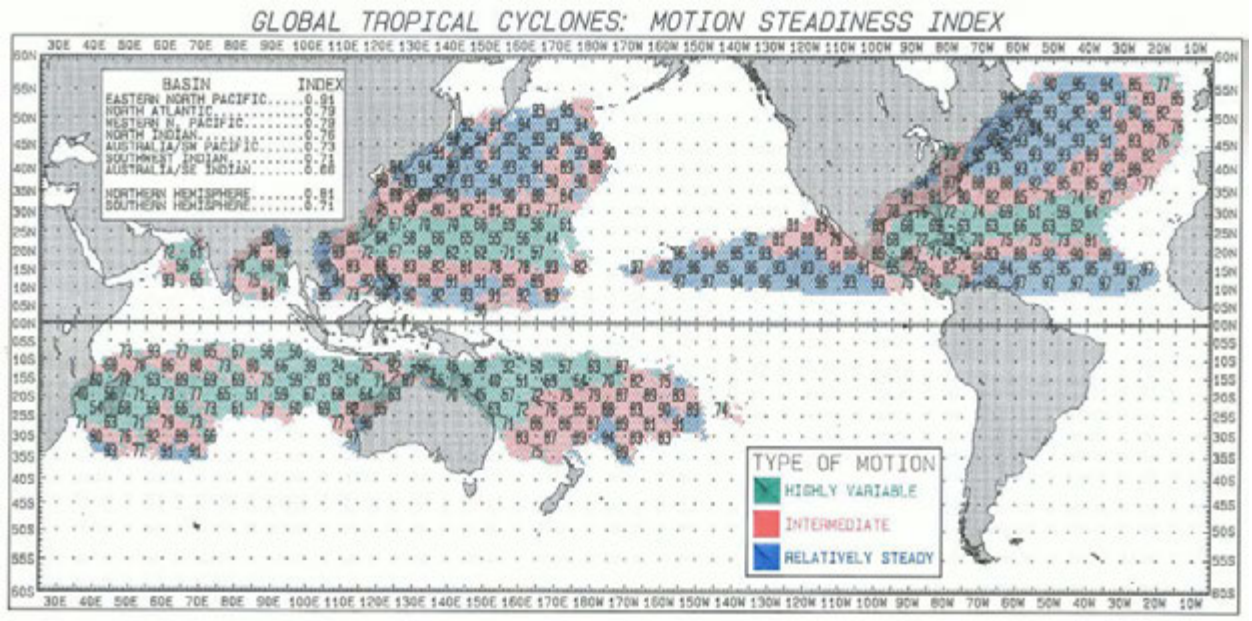

Figure 2.6. Steadiness index (SI) multiplied by 100. (click image for full size in new window)

Neumann (1981), defines a *forecast difficulty* index (FDI) based on residual errors from the CLIPER (Neumann, 1972) model. Pike and Neumann (1987) developed ad hoc CLIPER models to rank forecast difficulty for the various basins and their rankings are very similar to those given in the Fig. 2.6 table. Thus, both being a function of TC motion variability, the steadiness index is closely related to FDI. Forecast difficulty is mainly applicable to errors in statistical models. Recent error statistics (personal communication, M. Fiorino, 2008) on numerical model errors suggest that they are becoming more independent of the forecast difficulty concept.

2.3 Tabular data

2.3.1 Seasonal summaries

For the 30-year period, 1979-2008, Table 2.5 gives the number of tropical cyclones per season having maximum sustained winds of ≥34 kts (63 km h^{-1}) and ≥64 kts (118 km h^{-1}). Preparation of this table was problematic. In the previous edition of this Guide, the analogous table was based on a mixture of 1- and 10- minute averaged wind data. However, as stated in the introduction to this revised chapter, one of the goals is to present basin-comparable statistical data and the earlier wind-mixture is not consistent with that goal.

Thus, the decision was made to present two tables — one based on the 1-minute system (Table 2.5) and another on the 10-minute system (Table 2.6). Since 10-minute winds are not available for some basins, a decision was further made to multiply the best-track winds used in the construction of Table 2.5 by the usual factor 0.88 (see section 2.1.4) to estimate the 10-minute

<<Previous Next>>

winds. Errors introduced by this approximation are commensurate with the errors and uncertainties in specifying a representative surface wind.

Table 2.5. Based on 1-minute averaging, left cell entry gives seasonal totals of TC's with maximum winds ≥34 kts (63 km h^{-1}) and parenthetical entry with maximum winds ≥64 kts (118 km h^{-1}). Southern Hemisphere seasons begin and end 6-months prior to Northern Hemisphere seasons. Because some TC's traverse more than one basin, global totals (last column) are always less than or equal to the sums of the individual basins.

NH Season	North Atlantic	Eastern North Pacific	Western North Pacific	North Indian	Southwest Indian	Australia/ Southeast Indian	Australia/ Southwest Pacific	All Basins
1979	9(6)	10(6)	23(14)	5(2)	14(4)	7(2)	11(3)	74(37)
1980	11(9)	14(7)	24(15)	4(0)	14(9)	9(6)	10(4)	81(47)
1981	12(7))	15(8)	28(16)	3(2)	15(5)	9(5)	10(4)	89(47)
1982	6(2)	23(12)	26(19)	5(2)	14(7)	13(3)	7(5)	91(50)
1983	4(3)	21(12)	23(12)	3(0)	7(4)	4(2)	15(11)	77(44)
1984	13(5)	21(13))	27(16)	4(2)	17(7)	10(6)	9(3)	99(52)
1985	11(7)	23(13)	26(17)	6(0)	15(6)	12(8)	13(6)	102(56)
1986	6(4)	17(9)	28(19)	3(0)	15(8)	9(4)	10(6)	86(50)
1987	7(3)	20(10)	24(18)	8(0)	9(3)	6(4)	13(7)	87(45)
1988	12(6)	15(7)	26(14)	5(1)	13(7)	1(0)	7(5)	76(40)
1989	11(7)	17(9)	31(21))	3(1)	15(8)	6(4))	14(6)	95(56)
1990	14(8)	21(16)	31(21	2(1)	15(10)	7(5)	7(4)	93(64)
1991	8(4)	14(10)	30(20)	4(1)	10(6)	6(2)	4(3)	74(45)
1992	7(4)	27(16)	32(21)	11(3)	13(5)	6(4)	15(9)	105(60)
1993	8(4)	15(11)	30(21))	2(2)	13(4)	4(0)	13(8)	83(50)
1994	7(3)	20(10)	36(21)	5(1)	17(11)	9(4)	6(4)	96(53)
1995	19(11)	10(7)	26(15)	4(2)	12(7)	4(3)	5(3)	80(48)
1996	13(9)	9(5))	33(21)	8(4)	13(8)	10(5)	7(2)	89(54)
1997	8(3)	19(11)	31(23)	4(2)	18(11)	6(3)	16(9)	100(61)
1998	14(10)	13(9)	18(9)	8(5)	13(2)	7(3)	18(12)	90(50)
1999	12(8)	9(6)	24(11)	5(3)	15(5)	10(7)	11(3)	83(41)
2000	15(8)	19(6)	24(15)	4(1)	13(8)	10(7)	9(4)	89(46)
2001	15(9)	15(8)	29(20)	4(1)	10(7)	8(3)	5(2)	84(49)
2002	15(8)	12(6)	26(18)	5(0)	15(9)	4(1)	7(2)	83(42)
2003	16(7)	16(7)	22(17)	4(1)	14(9)	5(2)	10(7)	85(49)
2004	19(11)	15(9)	31(20)	5(2)	12(9)	5(3)	4(2)	84(51)
2005	28(15)	15(70	24(18)	6(0)	12(6)	9(2)	7(6)	99(53)
2006	10(5)	19(11)	22(14)	6(1)	9(3)	8(3)	8(5)	79(41)

<<Previous

Next>>

2007	16(7)	11(4)	22(16)	6(3)	10(8)	5(3)	8(4)	78(45)
2008	16(9)	16(7)	26(12)	6(1)	14(7)	7(3)	7(4)	91(43)
Sums	355(196	491(271)	803(514	148(44)	396(203)	216(107	286(153)	2623(1469)
Average	11.8(6.5)	16.4(9.0)	26.8(17.1)	4.9(1.5)	13.2(6.8)	7.2(3.6)	9.5(5.1)	87.4(49.0)
Std Dvn	4.8(2.9)	4.5(3.1)	4.0(3.5)	1.9(1.3)	2.5(2.3)	2.7(1.9)	3.7(2.6)	8.5(6.4)
Percent	13.2(13.2)	18.2(18.2)	29.8(34.5)	5.5(3.0)	14.7(13.7)	8.0(7.2)	10.6(10.3)	100.(100.)

<<Previous

Next>>

Table 2.6. Same as Table 2.5 except winds averaged over 10 minutes.

NH Season	North Atlantic	Eastern North Pacific	Western North Pacific	North Indian	Southwest Indian	Australia/ Southeast Indian	Australia / Southwest Pacific	All Basins
1979	9(6)	10(6)	23(14)	5(2)	14(4)	7(2)	11(3)	74(37)
1980	11(9)	14(7)	24(15)	4(0)	14(9)	9(6)	10(4)	81(47)
1981	12(7))	15(8)	28(16)	3(2)	15(5)	9(5)	10(4)	89(47)
1982	6(2)	23(12)	26(19)	5(2)	14(7)	13(3)	7(5)	91(50)
1983	4(3)	21(12)	23(12)	3(0)	7(4)	4(2)	15(11)	77(44)
1984	13(5)	21(13))	27(16)	4(2)	17(7)	10(6)	9(3)	99(52)
1985	11(7)	23(13)	26(17)	6(0)	15(6)	12(8)	13(6)	102(56)
1986	6(4)	17(9)	28(19)	3(0)	15(8)	9(4)	10(6)	86(50)
1987	7(3)	20(10)	24(18)	8(0)	9(3)	6(4)	13(7)	87(45)
1988	12(6)	15(7)	26(14)	5(1)	13(7)	1(0)	7(5)	76(40)
1989	11(7)	17(9)	31(21))	3(1)	15(8)	6(4))	14(6)	95(56)
1990	14(8)	21(16)	31(21	2(1)	15(10)	7(5)	7(4)	93(64)
1991	8(4)	14(10)	30(20)	4(1)	10(6)	6(2)	4(3)	74(45)
1992	7(4)	27(16)	32(21)	11(3)	13(5)	6(4)	15(9)	105(60)
1993	8(4)	15(11)	30(21))	2(2)	13(4)	4(0)	13(8)	83(50)
1994	7(3)	20(10)	36(21)	5(1)	17(11)	9(4)	6(4)	96(53)
1995	19(11)	10(7)	26(15)	4(2)	12(7)	4(3)	5(3)	80(48)
1996	13(9)	9(5))	33(21)	8(4)	13(8)	10(5)	7(2)	89(54)
1997	8(3)	19(11)	31(23)	4(2)	18(11)	6(3)	16(9)	100(61)
1998	14(10)	13(9)	18(9)	8(5)	13(2)	7(3)	18(12)	90(50)
1999	12(8)	9(6)	24(11)	5(3)	15(5)	10(7)	11(3)	83(41)
2000	15(8)	19(6)	24(15)	4(1)	13(8)	10(7)	9(4)	89(46)
2001	15(9)	15(8)	29(20)	4(1)	10(7)	8(3)	5(2)	84(49)
2002	15(8)	12(6)	26(18)	5(0)	15(9)	4(1)	7(2)	83(42)
2003	16(7)	16(7)	22(17)	4(1)	14(9)	5(2)	10(7)	85(49)
2004	19(11)	15(9)	31(20)	5(2)	12(9)	5(3)	4(2)	84(51)
2005	28(15)	15(7)	24(18)	6(0)	12(6)	9(2)	7(6)	99(53)
2006	10(5)	19(11)	22(14)	6(1)	9(3)	8(3)	8(5)	79(41)
2007	16(7)	11(4)	22(16)	6(3)	10(8)	5(3)	8(4)	78(45)
2008	16(9)	16(7)	26(12)	6(1)	14(7)	7(3)	7(4)	91(43)
Sums	355(196)	491(271)	803(514	148(44)	396(203)	216(107	286(153)	2623(1469)
Average /td>	11.8(6.5)	16.4(9.0)	26.8(17.1)	4.9(1.5)	13.2(6.8)	7.2(3.6)	9.5(5.1)	87.4(49.0)
Std Dvn	4.8(2.9)	4.5(3.1)	4.0(3.5)	1.9(1.3)	2.5(2.3)	2.7(1.9)	3.7(2.6)	8.5(6.4)
Percent	13.2(13.2)	18.2(18.2)	29.8(34.5)	5.5(3.0)	14.7(13.7)	8.0(7.2)	10.6(10.3)	100.(100.)

<<Previous

Next>>

Other than the use of the 0.88 conversion factor, there are several reasons why the data listed in these tables may differ from data maintained by other groups. Pre-1990 Table 2.5 data are a composite (Neumann, 1999) of best-tracks from various RSMC's and the Australian Bureau of Meteorology; later data are from JTWC and NHC. Another reason for differences between Table 2.5 data and that maintained by the various Centers could be related to basin bounds as stated in Table 2.2. Still other reasons could be related to local counting procedure. For example, the 1999 JTWC Annual TC Report lists 12 tropical storms and 12 typhoons or super typhoons in the western North Pacific for that year, whereas the Neumann data set gives only 11 typhoons or super-typhoons. Perhaps this is due to a different interpretation of 1999 TC DORA's intensity as it moved northwestward across the dateline from the central North Pacific basin to the western North Pacific basin.

2.3.2 Other comments on seasonal summaries

In addition to basin frequencies, Table 2.5 and 2.6 give global totals and it might be noted that these totals are typically less than the sum of individual basin totals. As mentioned in the table heading, this is due to some TC's traversing more than one basin. For example, 1999 DAMIEN, in the Australia/SE Indian Ocean basin moved westward and was renamed BIRENDA by the Mauritius Meteorological Service. This is only counted as a single TC. Another example was hurricane DORA, cited in the previous paragraph. The annual average number of TC's having maximum winds at least 34 kts (63 km h^{-1}) and summed in this manner is given as 87.4 in Table 2.5 and 79.7 in Table 2.6. (For the same 30-year period (1979-2008) and based on 10-min wind averaging, IBTrACS (Kruk et al., 2008) gives a seasonal average of 78.2 (37.4) TC's.) Before making further interpretations of data given in these tables, it should be noted that the beginning and ending times of SH seasons are 6-months prior to NH seasons.

The standard deviation of global totals is considerably higher than that of individual basins. Also, as would be expected, the western North Pacific TC basin is the largest contributor to the global totals while the North Indian basin is the smallest.

From Table 2.5, it is noted that the annual number of global tropical cyclones shows wide variation. In 1991, only 74 TC's were identified worldwide, while, for the following year, the count rose to 105. As noted earlier, the global standard deviation (8.5 TC's) of seasonal totals is greater than the standard deviation for individual basins.

2.4 Meridional profiles

Meridional profiles of zonally averaged TC parameters for each of the seven basins defined in Table 2.2 are presented in Figs. 2.7 through 2.10. The data for each basin were averaged zonally for 2-degree latitude bands centered at odd latitudes from 1° to 55°N. The total number of TC's included in the analysis are given in the inset as "NSTMS=nnn", while the number of cyclones passing within each latitude band is given in the column labeled "number of cyclones". Thus, for

the North Atlantic basin (Fig. 2.7) there were 1145 TC's used in the analyses and 240 of them passed through the 12°-14°N latitude band. Only those bands having at least 10 cases were included in the analyses.

The meridional profiles show average **u** (zonal speed component), **v** (meridional speed component) and **s** (scalar speed) within each latitude band while arrows depict vector heading with length proportional to scalar speed. In general, all increase with increasing latitude. However, there are some exceptions in the more polar and equatorial regions. In the Atlantic or example, south of about 22°N, average scalar speeds increase equatorward and, at high latitudes, there is some decrease in the u-component. Over the eastern North Pacific, recurving and accelerating TC's often make landfall over Mexico and rapidly dissipate. This feature shows up as somewhat of a discontinuity near 29°N. Because of fewer TC movements into the more poleward latitudes, SH cyclones, on average, have lower translational speeds than those of the NH. Other features can be noted on individual charts.

2.4.1 Translational motion

The inset on each figure gives the latitude of zero zonal motion (U_0).In basins that exhibit a classical recurvature pattern such as the North Atlantic, the western North Pacific and, to some extent, the southwest Indian Ocean basin, this can be interpreted as the average latitude of recurvature into the westerlies. However, the two Australian basins lack the classical recurvature pattern and U_0 has no significant meaning in that regard.

Also specified on each chart is the average wind (WBAR), here defined as the basin-wide average of all 34 kt (63 km h<sup-1< sup="">) six-hourly best-track winds. For a number of reasons, this is a rather frail statistic. However, when used in conjunction with the same statistic for each two-degree latitude band (W_j), it provides a *maximum wind index* (W_j/WBAR), where some of the fragility cancels out. For the Atlantic basin, this index varies from 0.71 at the lowest latitude band to 1.05 at the latitude band centered at 27°N. The maximum wind zone for this basin is located just equatorward of the average recurvature latitude (U_0), 27.6°N. A similar relationship between recurvature latitude and maximum wind zone can be noted for the other basins having the classical recurvature pattern (western North Pacific and southwest Indian Ocean) but not for the other basins. For the western North Pacific, this relationship was pointed out by Riehl (1972). Later investigators (Evans and McKinley, 1998; Knaff, 2009) also point out that the relationship, on the average, is valid in some basins but not in others and that it is somewhat dependent on the TC intensity.</sup-1<></sup-1<>

2.4.2 Meridional values of steadiness index

As previously discussed and portrayed in Fig. 2.6, Figs. 2.7 through 2.10 also give meridional values of the steadiness index as was displayed globally on Fig. 2.6. For basins having the classical recurvature pattern, steadiness values are lowest in the recurvature latitudes. As pointed out earlier, steadiness values are lower in the SH than in the NH. For the

Australia/southeast Indian basin (Fig. 2.9), SI values are particularly low with averages of 0.40 being noted between latitudes 10° to 12°S.

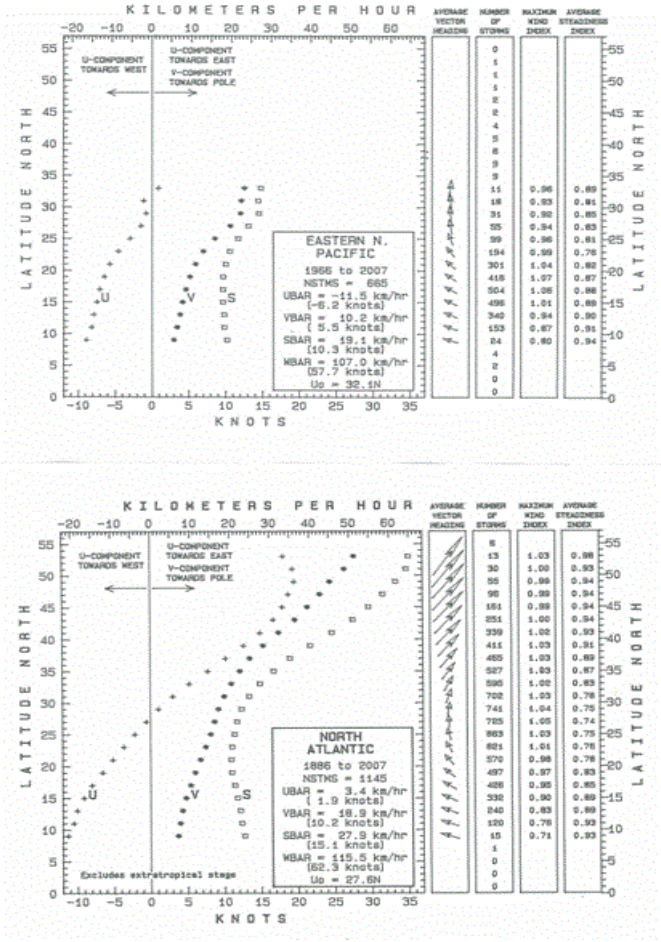

Figure 2.7. Meridional values of the steadiness index for the E. North Pacific and North Atlantic basins

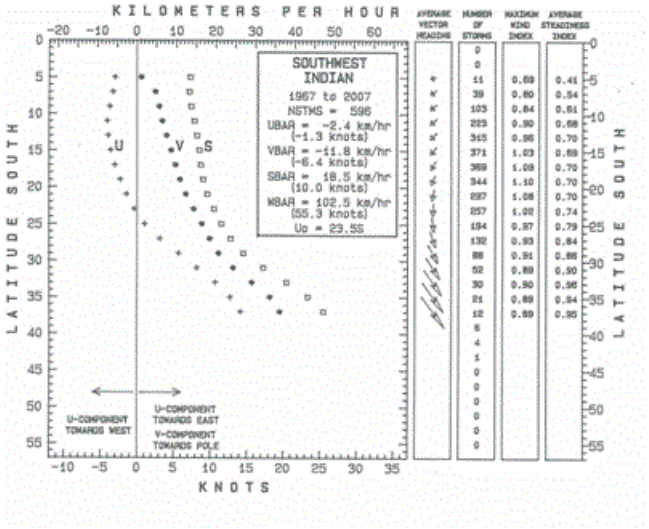

<<Previous

Next>>

Figure 2.8. Meridional values of the steadiness index for the Southwest Indian basin.

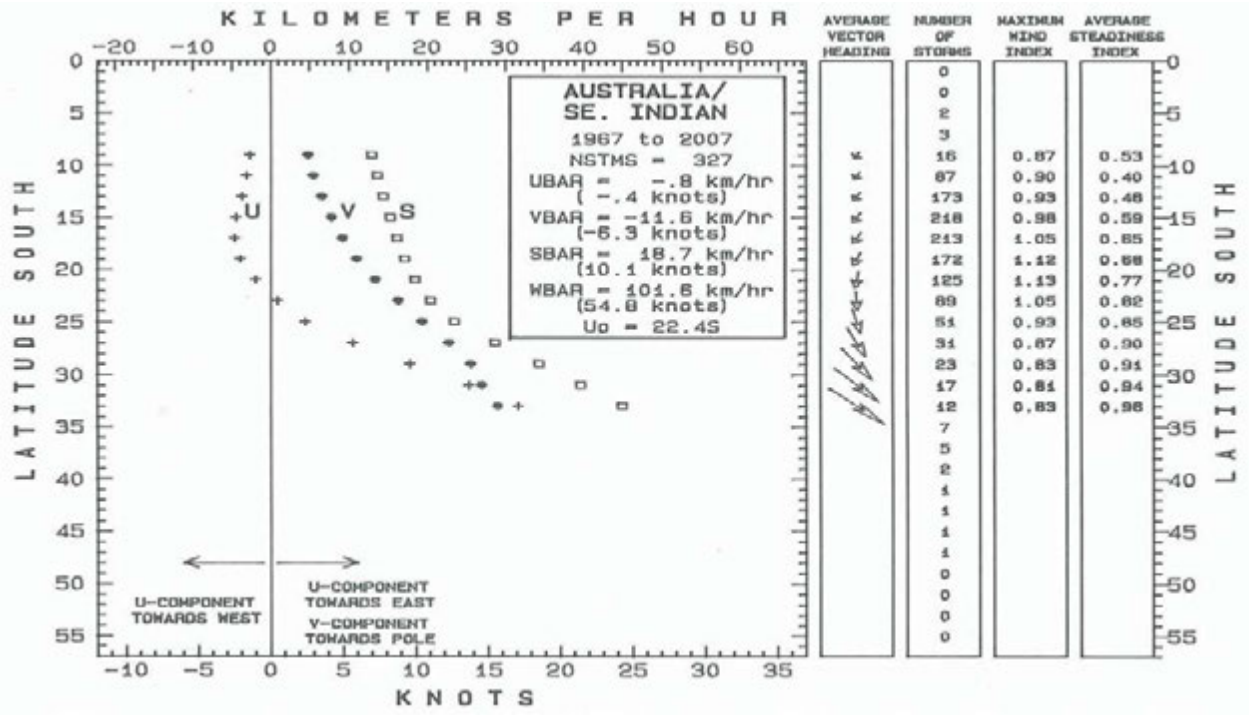

Figure 2.9. Meridional values of the steadiness index for the Australia / SE Indian basins.

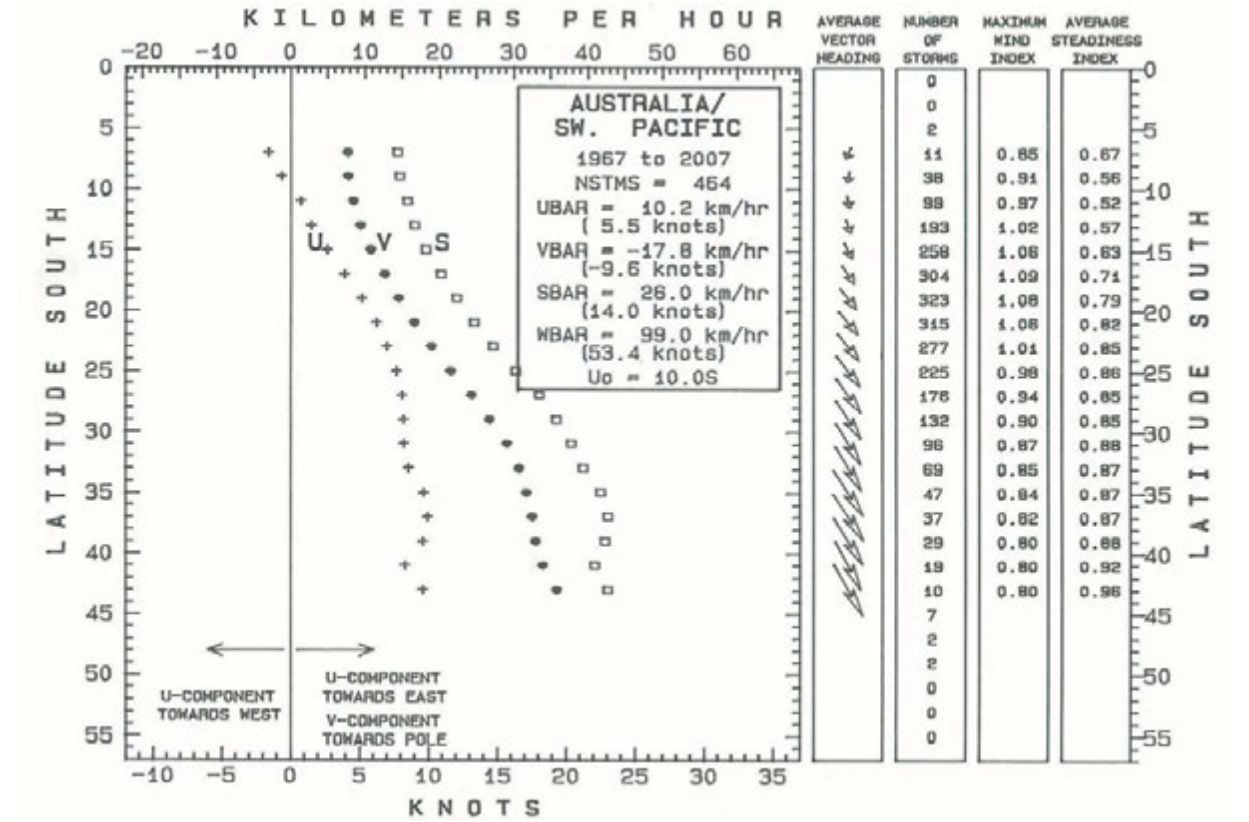

<<Previous

Next>>

Figure 2.10. Meridional values of the steadiness index for the Australia / SW Pacific basins.

2.5 Intra-seasonal TC occurrence

Using the same global data set described earlier, Figs. 2.11 through 2.13 (shown on the next page) address the average day-to-day variation in tropical cyclone occurrence. Several authors (Holland, 1981; Murphy, 1988; Harper et al., 2008; Landsea, 1993) point out that not all TC's were detected in the pre-satellite era and that their intensities were under- or even over-estimated. Accordingly, there may be somewhat more tropical storm or hurricane area than shown on these charts. The data were smoothed using a moving-average period of 15-days. For very long periods of record, McAdie et al. (2008) find that, for charts of this type, a 9-day period is optimal for removing random data fluctuations while preserving known seasonal variations. However, the longer 15-day moving average used here is more applicable to relatively short period of records for the SH. The unit of measurement is *number of tropical cyclones per 100 years*. Use of this unit bypasses the problem of dealing with dissimilar periods of record.

In preparation of these figures, multiple TC occurrences on single days were included in the overall totals. Thus, the occurrence of three TC's on a given date and year would yield the same average as a single TC on the same date for each of three years. This counting methodology needs to be considered when making further interpretations of these data.

The Poisson probability function is useful in estimating the probability of, 0, 1, 2,...n, TC's occurring on single days (Xue and Neumann, 1984a). The Poisson distribution is given by $P(x) = e^{-m}m^x/x!$, where m is the mean occurrence over the desired period and x is the number of occurrences. For example, for the Australia/SW Pacific basin, the number of TC's per 100 years on 27 February is given on Fig. 2.12 as 55.9. According to the Poisson distribution*, this gives the theoretical probability ($0 \leq p \leq 1$) of 0, 1, 2 and ≥1 TC's on this date as 0.57, 0.32, 0.09 and 0.43, respectively.

These figures reveal much of the temporal character of the tropical cyclone activity over the various basins. Obviously, the seasonal shift between the two hemispheres is clearly shown. The western North Pacific is the only basin showing activity throughout the year but with a distinct minimum in mid-February. The season is also quite lengthy over the southwest Indian basin. The North Atlantic shows a sharp maximum near 10 September and another weak maximum around 10 October caused by the activation of a separate genesis region over the western Caribbean area. Other basins such as the North Indian exhibit more of a bimodal pattern caused by seasonal migration of the monsoon trough. Other than the above, it is uncertain whether some of the small-scale patterns are real or are due to an insufficient period of record. Additional details are provided by Frank (1987).

By summing individual basin daily values, Fig. 2.13 shows the global tropical cyclone daily occurrence pattern. The maximum near 10 Sept. is related to the greater NH activity while the

<<Previous Next>>

secondary maximum centered about 10 February is due to lessor SH activity. As would be expected, the two peaks are exactly six months apart. Minimum global activity is noted in late April/early May. In Fig. 2.13, there is also a suggestion that the percentage of tropical cyclones reaching the 64 kt threshold is somewhat greater in the Northern Hemisphere. More details for the Atlantic can be found in McAdie et al. (2008) and for the Australian area in BoM (1978).

$P(x) = e^{-m}.m^{x}/x!$, where m is mean occurrence over desired period and x is number of occurrences.

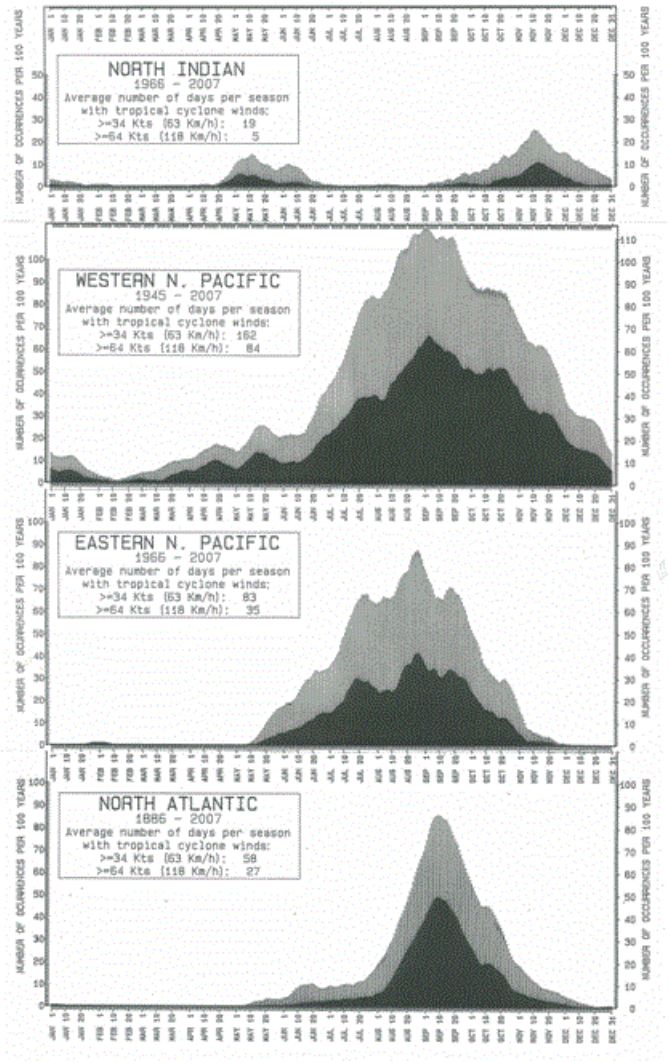

Figure 2.11. Average day-to-day variation in tropical cyclone (TC) occurrence for Northern Hemisphere basins. Gray area indicates TCs >34 kt (>63 km/hr) and black area indicates TCs >63 kt (>118 km/hr).

<<Previous

Next>>

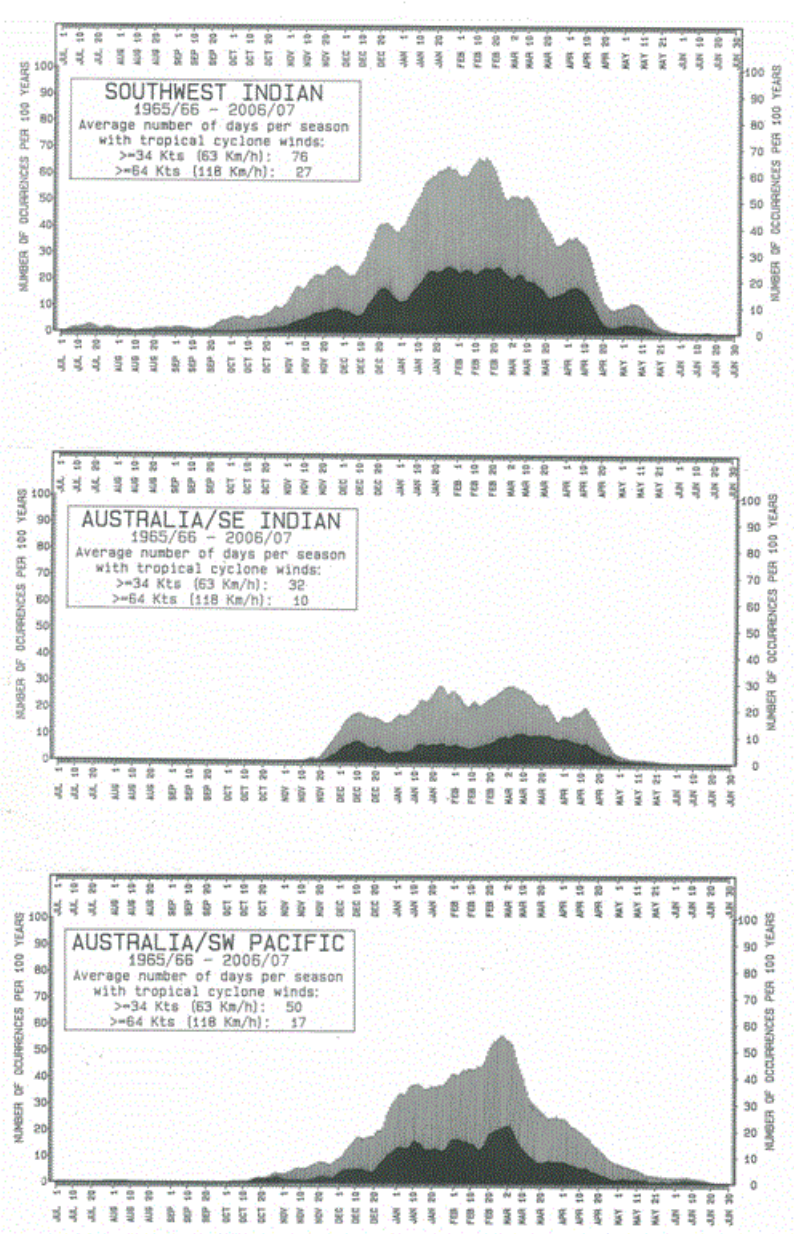

Figure 2.12. Average day-to-day variation in tropical cyclone (TC) occurrence for Southern Hemisphere basins. Gray area indicates TCs >34 kt (>63 km/hr) and black area indicates TCs >63 kt (>118 km/hr).

<<Previous

Next>>

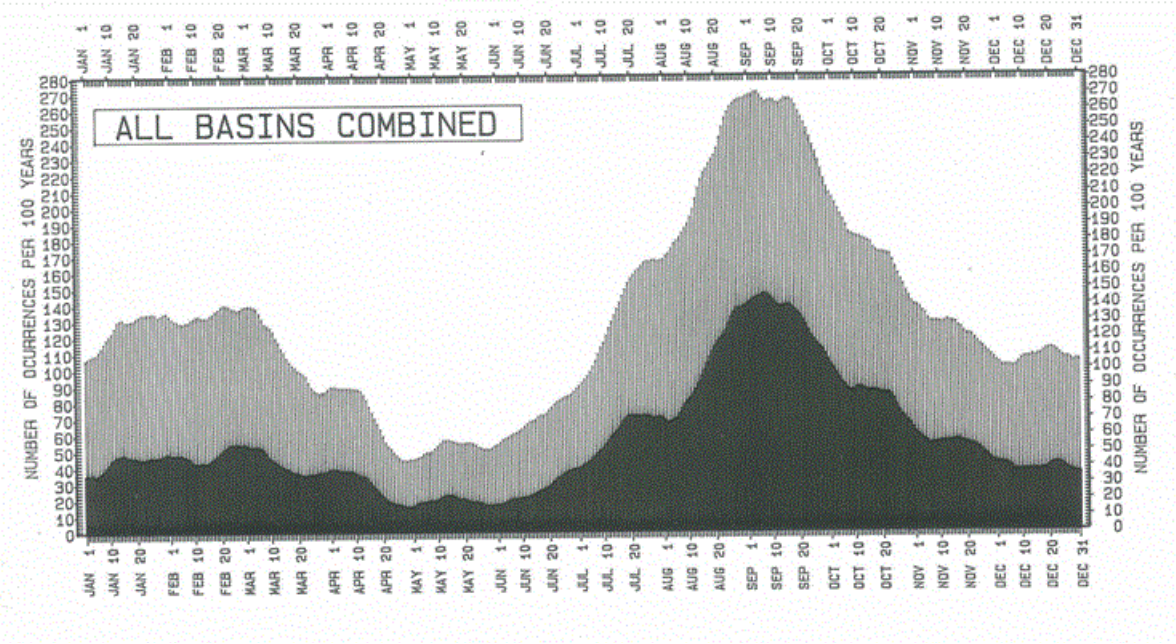

Figure 2.13. Average global day-to-day variation in tropical cyclone (TC) occurrence for all basins combined. Gray area indicates TCs >34 kt (>63 km/hr) and black area indicates TCs >63 kt (>118 km/hr).

2.6 Some statistical considerations

Further interpretation of climatic data often involves fitting to parent probability distributions or mathematical functions. This allows inferences to be made about gaps in the data or in making inferences beyond the range of the observational evidence. However, there are many pitfalls here. There is always the danger of selecting the wrong mathematical relationship or of trying to fit a multimodal set of data with a unimodal function. As stated by the pre-computer-age statistician Mills (1955), fitting of data to a mathematical function or distribution is often done on the grounds of "practicality or expedience". To this could be added: on the grounds of "convention" (Wilks, 2008, personal communication). If the parent distribution is difficult to identify and a long period of some event is available, it may be profitable to use empirical rather than mathematical probabilities.

Detailed discussion of statistical applications is well beyond the scope of this chapter. Only some of the more important issues, as they relate to TC's, will be discussed here. Readers are referred to the above authors for a more in-depth discussion.

2.6.1 Binomial and Poisson distributions

Building codes are often based on *n*-year wind events where *n* is often taken as 50- or 100-years. For structures with a high degree of hazard, such as nuclear power plants, much longer periods for some components of the construction are used. An *n*-year wind event is a wind

<<Previous

Next>>

value that is equaled or exceeded on the average every *n* years. A closely related statistic is the recurrence interval or return-period, defined as the average number of years between an event. If this average is 50 years, then it is a 50-year event.

If, over a 50-year period, an event occurs for the first three years and not at all for the next 47 years or if it occurs at 25-, 15- and 10-year intervals, the average return year period of 50/3 or 16.7 years would be the same. Thus, *n*-year events need not occur every *n* years.

For randomly occurring events, it can be shown exactly by the binomial distribution and to a close approximation by the Poisson distribution that the percentage probability of an *n*-year event occurring at least once in *n* years is 63.4%; in 2*n* years, 86.6%; in 5*n* years, 99.3%. The chance of the event not occurring would be 100% minus those values. Meteorological events are often associated with large-scale atmospheric periodicities, which tend to lock in specific atmospheric patterns, such that the randomness requirement may be somewhat invalidated. However, experience has shown that the Poisson distribution gives reasonable TC event estimates.

2.6.2 Mixed distributions

2.6.2.1 TC motion (bivariate normal distribution)

One of the more useful distributions in tropical cyclone work is the bivariate normal. Five parameters are needed to define the distribution: the means of the x and y components, their standard deviations and the linear correlation coefficient between x and y components. The distribution was illustrated and briefly discussed in section 2.2.4. It is often used to describe tropical cyclone motion, forecast errors and strike probabilities (Sheets, 1984). A pitfall often ignored when fitting bivariate data thereto is the possibility that the data are bimodal rather than unimodal (Crutcher and Joiner, 1977).

A good example of the latter problem is given by Crutcher et al. (1982). The authors show that tropical cyclone forecast errors for the Atlantic basin come from more than one bivariate normal distribution. They also show that clustering algorithms can be used to sort the data into homogeneous sets.

Another example of this mixture problem can be found in areas where tropical cyclone tracks tend to diverge in a bimodal pattern. In the Atlantic, this occurs east of Barbados where tracks tend to move either with more of a poleward component north of the Leeward Islands or to continue westward into the Caribbean Sea. To a lesser extent, this same divergent pattern occurs off the northwest coast of Australia where some TC's continue westward or recurve southward.

2.6.2.2 TC wind (Weibull distribution)

The Weibull distribution (Tsokos, 1972; Abernethy et al., 1983) can be used to describe tropical cyclone maximum winds (Georgiou, 1985). However, one problem to be addressed in fitting TC maximum winds to this distribution (Neumann, 1987) is that the right tail extends to infinity whereas there are environmental constraints for TC maximum sustained winds going beyond certain limits. This concept of maximum possible intensity (MPI) is discussed by Emanuel (1986).

In the previous section, the problem of mixed data being fitted to the bivariate normal distribution was discussed. The same potential problem exists in fitting to other distributions such as the Weibull. This is illustrated in Fig. 2.14 where maximum wind data at three sites are fitted to this distribution. In the top panel, the fit is visually quite good and the mathematical probabilities can be used in place of the empirical values. At this coastal site, intensity data is reasonably reliable and the slight wind misfit could well have been within wind estimation error. Here, TC's make landfall from a unimodal direction distribution.

The Miami wind data depicted in the center panel of Fig. 2.14 are also quite reliable and the data suggest a secondary maximum wind peak in the class-intervals near 100 knots. This bimodal maximum wind distribution is probably related to the fact that the TC approach direction at this location mid-July through mid-September is from the south to east and more from the southwest in the early and late portions of the North Atlantic season. Making random selections from this distribution, as is often done in risk analysis, would underestimate winds in the 84 to 124 kt (156-230 km h^{-1}) range. Here, it might be necessary to make seasonal fits to the wind data.

In the lower panel of Fig. 2.14, for whatever the reason, the fit is completely unsatisfactory. Without further analyses, the Weibull function could not be used for a wind analysis at this site.

<<Previous

Next>>

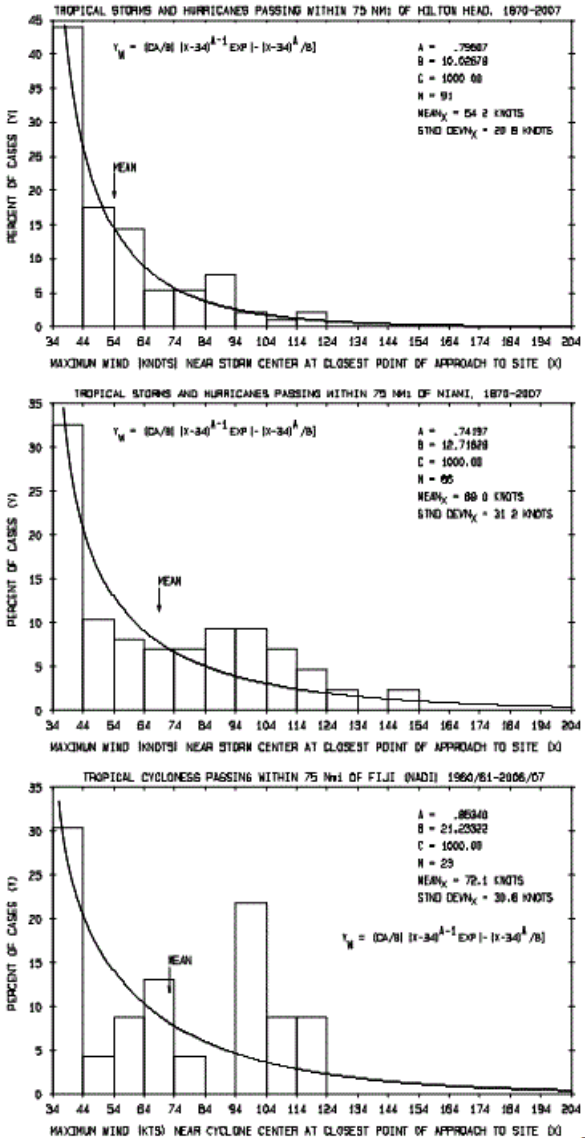

Figure 2.14. Example of good (top), marginal (center) and poor (bottom) fits of TC maximum wind to a Weibull distribution.

2.6.3 Other TC related distributions

Insofar as TC's are concerned, radius of maximum winds (RMW) data are often fitted to a log-normal distribution (Neumann, 1987; Georgiou, 1985; Batts et al., 1980). On the average, RMW is directly proportional to latitude and inversely proportional to TC intensity. Although the explained variance is rather small, RMW is often taken as an empirical function of these two TC parameters (Neumann, 1987).

Finally, the Gamma distribution (Hahn and Shapiro, 1967) is often used to describe variables bounded on one end by zero but unbounded on the other end. Thus, the distribution is often

<<Previous

Next>>

used to describe rainfall amounts. As discussed by Neumann (1987), it could also be used in place of the Weibull distribution for TC winds.

2.6.4 Additional remarks

Many statistical applications require specification of the sample size. Because of serial correlation in meteorological time series, the true (uncorrelated) sample size is typically much less than the apparent sample size. Some of the TC aspects of this problem are discussed by Neumann (1979). However, the issue is quite complex and recommended references are to an old textbook on statistical methods in the social and economic sciences (Mills, 1955) and a new textbook on statistical methods in the atmospheric sciences (Wilks, 2006).

In the pre-computer age, fitting of large masses of data to mathematical functions and statistical distributions was tedious. However, the process was associated with a close scrutiny of the data and errors, inconsistencies and biases were often noted. TC data, now typically estimated or remotely sensed, are particularly vulnerable to these data problems and with modern computer technology, are easily overlooked. Accordingly, many of the discussions in this Chapter called attention to the data issue. As stated by the pre-computer age statistician Mills, (1955), "Wisdom in the selection of functions, time-units, strategic periods, etc., requires some understanding of the ground plan of nature in the particular field of study, as well as competence in the application of statistical techniques. The task of analysis is never purely mechanical."

The chapter is concluded with a blank section for inclusion of regional climatologies by local forecast offices.

2.7 References

Abernethy, R.B. J.E. Breneman, C.H. Medlin and G.L. Reinman, 1983: *Weibull Analysis Handbook*, AFWAL-TR-2079,USAF, Aero Propulsion Laboratory, Wright-Patterson AFB, 228 pp.

Akima, H., 1970: A new method of interpolation and smooth curve fitting based on local prodedures.*J. Assoc. Computing Mach.* **17**, 589-602.

Batts, M.E., M.R.Cordes, L.R. Russell, J.R. Shaver and E. Simiu, 1980: Hurricane wind speeds in the United States. *NBS Building Science Series* 124 , 41 pp.

Bell, G. D., M. S. Halpert, R. C. Schnell , R. W. Higgins, J. Lawrimore, V. E. Kousky, R. Tinker, W. Thiaw , M. Chelliah, and A. Artusa, 2000: Climate Assessment for 1999. *Bull. Amer.* Met. Soc., June 2000, pp. S1-S50.

Brand, S. and J.W. Blelloch, 1974: Changes in the Characteristics of Typhoons Crossing the Island of Taiwan. *Mon. Wea. Rev.,* **102**, 708-713

<<Previous Next>>

BoM, 1978: *The Australian Tropical Cyclone Forecasting Manual.* (Ed. A. B. Neal & G. J. Holland) Bureau of Meteorology, Melbourne, Australia, 274 pp.

Chenoweth, M. And C. Landsea, 2004: The San Diego hurricane of 2 October, 1858. *Bull. Amer. Meteor. Soc.*, **85**, 1689-1697.

Crutcher .H. L. and R. L. Joiner, 1977: Separation of Mixed Data Sets into Homogeneous Sets, *NOAA Technical Report* EDIS 19, Asheville, NC., 167 pp.

Crutcher, H. L., C. J. Neumann and J. R. Pelissier, 1982: Tropical cyclone forecast errors and the multinormal bivariate normal distribution. J. *Appl. Meteor*, **21**, 978-989.

Crutcher , H, L. and R. G. Quayle, 1974: *Mariner's worldwide guide to tropical storms at sea*. National Climatic Center and U. S. Navy, Asheville, NC., 114 pps. + 312 charts

Elsberry, R. L, 1987: Tropical Cyclone Motion. *A global view of tropical cyclones*. (ED. R.L. Elsberry), ONR Marine Meteorology Program, Arlington, VA, 91-128.

Emanuel, K.A., 1986: An Air-sea Interaction Theory for Tropical Cyclones. Part I. *J. Atmos. Sci.* **42**, 586-604.

Evans, J. L. and K. McKinley, 1998: Relative Timing of Tropical Storm Lifetime Maximum Intensity and Track Recurvature. *Meteorol. Atmos. Phys.,* **65,** 241-245.

Frank, W. M., 1987 : Tropical Cyclone Development. *A global view of tropical cyclones.*(Ed. R. L. Elsberry), ONR Marine Meteorology Program, Arlington, VA, 53-90

Georgiou, P.N., 1985: Design Wind Speeds in Tropical Cyclone Prone Regions. University of Western Ontario *Research Report* BLWT-2-1985, London, Ontario, Canada, 295pp.

Guard, C. P. and M. A. Lander, 1996: A wind-pressure relationahip for midget TC's in the western North Pacific. *Annual Tropical Cyclone Report (ACTR), JTWC*, page 311.

Hahn, G.J. and S.S. Shapiro, 1967: *Statistical Models in Engineering*. John Wiley & Sons, New York, NY, 354 pp.

Harper, B. A., S. A. Stroud, M. McCormick and S. West, 2008: A review of historical tropical cyclone intensity in Northwestern Australia and implications for climate change trend analysis. Aust. Met. Mag . 59, 121-141. .

Holland, G. J., 1981: On Quality of the Australian Tropical Cyclone Data Base. *Aus. Met. Mag.,* **29**, 169-181.

<<Previous

Next>>

Hope, J. R., and C. J. Neumann, 1968: Probability of Tropical Cyclone Induced Winds at Cape Kennedy. *ESSA Technical Memorandum* SOS-1. 67 pp.

Hope, J. R. and C. J. Neumann, 1971: Computer methods applied to Atlantic area tropical cyclone climatology. *Mariner's Wea. Log*, **15**, 272-278.

Hsu, S.A., and B.W. Blanchard, 2008: Tropical Cyclone Destructive Potential by Integrated Kinetic Energy. *Bull. Amer. Meteor. Soc.*, **89**, pp. 1575-1576.

Kruk, M. C., K. R. Knapp, D. H. Levinson and J. P. Kossin (2008), National Climatic Data Center Global Tropical Cyclone Stewardship. *Preprints*, 28th Conference on Hurricanes and Tropical Meteorology, Orlando, AM S

Knaff, J.A., and R. M. Zehr, 2007: Re-examination of tropical cyclone wind-pressure relationships. *Wea. And Fcstng.*, 22, 71-78.

Knaff, J. A., 2008: Knaff, J. A. 2009, Revisiting the maximum intensity of recurving tropical cyclones. *Int. J. Climatol.,* **29** 827-837.

Landsea, C. W., C. Anderson, N. Charles, G. Clark, J. Dunion, J. Partagás, P. Hungerford, C. Neumann and M. Zimmer, 2003: "The Atlantic hurricane database re-analysis project." Chapter 7, *Hurricanes and Typhoons, Past, Present and Future*, R.J. Murnane and K. B. Liu, Editors, CLandsea, C. W., 1993: A Climatology of Intense (or Major) Hurricanes. *Mon. Wea. Rev.*, **121**, 1703-1713.

McAdie, C. J., C. W. Landsea, C. J. Neumann, J. E. David, E. S. Blake and G. R. Hammer 2008: Tropical cyclones of the North Atlantic Ocean, 1851-2006. *Historical Climatology Series 6-2*. NOAA, National Climatic Data Center,

Mills, F.C., 1955: *Statistical Methods*. Holt, Rinehart and Winston, New York, NY, 842 pp

Murnane, R. J., 2004: Chapter 9, page 252 of *Hurricanes and typhoons, past, present and future*. Richard J. Murnane and Kam-Biu Liu, editors. Columbia University Press, 462 pps.

Murphy, K., 1988: Correspondence, Aust. *Met. Mag.*, **36**, 227-228.

Neumann, C. J.,1952: *Wind estimations from Aerial Observations of Sea Conditions*. USN Weather Squadron Two (VJ-2), NAS, Jacksonville FL., 26 pp. (limited distribution)

Neumann, C. J., 1972: An alternate to the HURRAN tropical cyclone forecast system. *NOAA Technical Memorandum* NWS SR-62., 24 pp.

<<Previous

Next>>

Neumann, C.J., 1979: *Operational techniques for forecasting tropical tyclone tntensity and movement.*, Chapter 4, World Meteorological Organization No. 528, pp. 4.21- 4.25 + appendices.

Neumann, C.J., 1981: Trends in forecasting the tracks of Atlantic tropical cyclones. *Bull. Amer. Met. Soc.*, **62**, 1473-1485.

Neumann, C. J., 1987: The National Hurricane Center risk analysis program (HURISK).*NOAA Technical Memorandum* NHC38, 56 pps.

Neumann, C.J., 1993: A global guide to tropical cyclone forecasting, Chapter 1.WMO *TD/560, pps. 1.1-1.42*

Neumann, C.J., 1996: *Minutes of the 50th Indepartmental Hurricane Conference*, U.S. Department of Commerce, NOAA, pp 1-2, Research presentations.

Neumann, C.J., 1999: The HURISK model: an adaptation for the Southern Hemisphere. SAIC Contract Report N00014-96-C-6015., Science Applications International Corporation, Monterey, CA, 53 pp.

Neumann, C.J., 2000: The Atlantic HURISK model: Adaptation to other tropical cyclone basins. Preprints, 24th Conf. on Hurricanes and Tropical Meteorology, Ft. Lauderdale, FL., Amer. Meteor. Soc., 549-550.

Pike, A.C. and C. J. Neumann, 1987: The variation of track forecast difficulty among tropical cyclone basins. *Wea and Fcstng.*, Vol. 2, No. 3, 237-241.

Powell, M.D. and T.A. Reinhold, 2007: Tropical cyclone destructive potential by integrated kinetic energy. *Bull. Amer. Meteor. Soc.*, **88**, 513-526.

Riehl, H. , (1972): Intensity of recurved typhoons. J. *Appl. Met.*, **11**, 613-615.

Sheets, R.C., 1984: The National Weather Service Hurricane Probability Program. *NOAA Technical Report* NWS 37, 70 pp.

Taylor, K.E., 1986: An analysis of the biases in traditional cyclone frequency maps. *Mon. Wea. Rev.*, Vol. 114, No. 8, 1481-1490

Tsokos, C.P. 1972: Probability Distributions: An Introduction to Probability Theory with Applications. Belmont, CA: Duxbury Press

Wilks, D. S. , 2006: *Statistical Methods in the Atmospheric Sciences*. 2nd Edition, Academic Press, 627 pp.

Xue, Z., and C.J. Neumann, 1984a: Frequency and motion of western North Pacific tropical cyclones. *NOAA Technical Memorandum NWS* NHC23, 84 pp.

<<Previous

Next>>

Xue, Z., and C. J. Neumann, 1984b: A new frequency and motion climatology of western North Pacific tropical cyclones. Preprints, AMS 15th Conf. On Hurr. and Trop. Meteor., pp.107-114.

Yeh, T,-C. and R. L. Elsberry, 1993: Interaction of typhoons with the Taiwan orography. *Mon. Wea. Rev.*, **121**, 3193-3212.

Zehnder, J. A., 1993: The influence of large-scale topography on barotropic vortex motion. *J. Atmos. Sci.* **50**, 2519-2532.

<<Previous

Next>>